Supporting Information

On-demand and tunable dual wavelength release of antibody using light-responsive hydrogels

Paige J. LeValley[1], Bryan P. Sutherland[2], Jennifer Jaje[3], Sandra Gibbs[3], R. Mark Jones[3,+], Rikhav P. Gala[3], Christopher J. Kloxin[1,2], Kristi L. Kiick[2,*], April M. Kloxin[1,2,*]

[1]Department of Chemical and Biomolecular Engineering, University of Delaware, Newark, DE, United States

[2]Department of Material Science and Engineering, University of Delaware, Newark, DE, United States

[3]Fraunhofer USA Center for Molecular Biotechnology (CMB), Newark, DE, United States

+ current address: Charles River Laboratories, Malvern, PA 19355, United States

** Co-corresponding Authors: Kristi L. Kiick kiick@udel.edu and April M. Kloxin akloxin@udel.edu*

Table of Contents

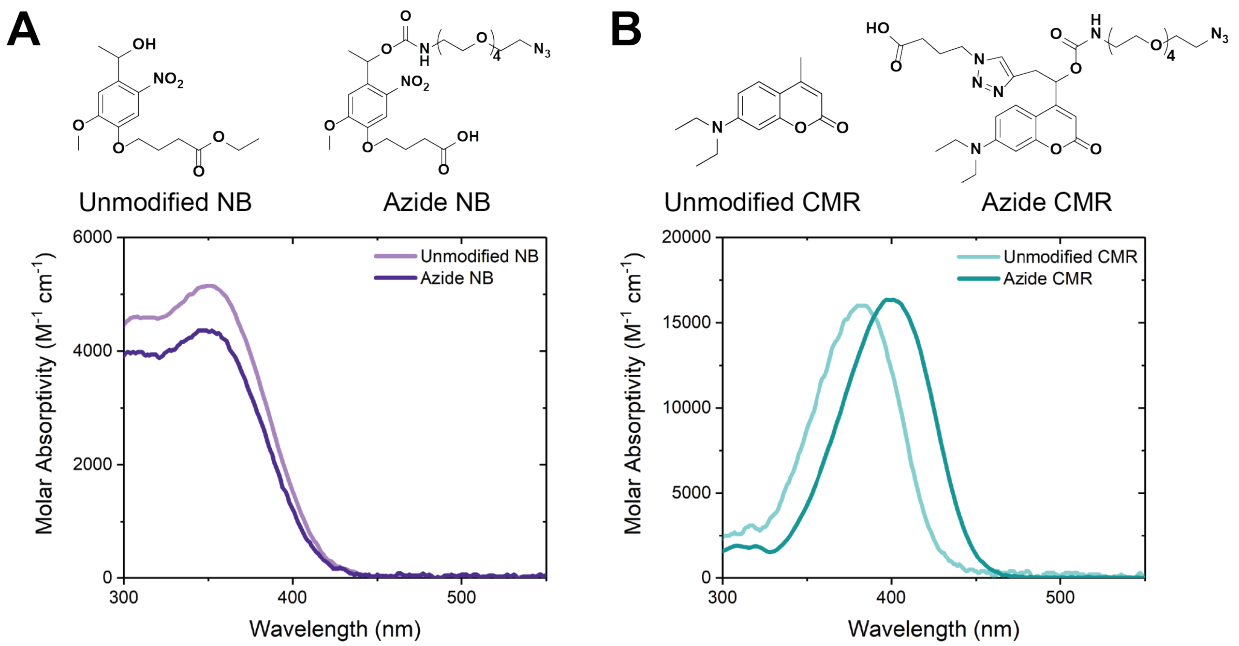

Figure S1. *Molar absorptivity of NB and CMR moieties.* The molar absorptivity of the small molecule (A) unmodified NB compared to NB-azide and (B) unmodified CMR compared to CMR-azide moieties was determined using UV-Vis spectrophotometry. There were only minimal observable differences in the molar absorptivity between the unmodified and azide functionalized NB and CMR molecules indicating that the functionalization procedure used did not detrimentally affect the light absorbance properties of the respective photolabile moieties.

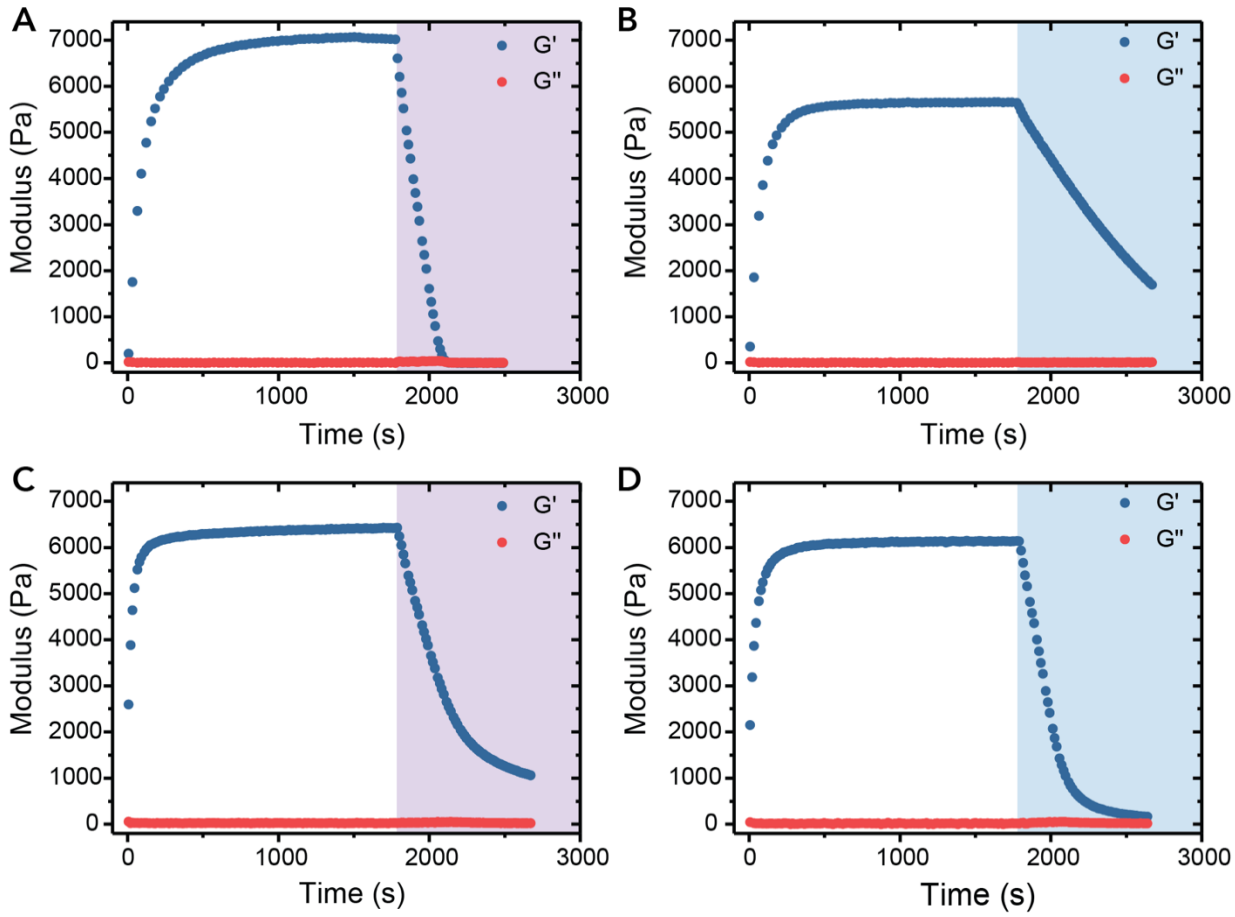

Figure S2. *Rheology of nitrobenzyl (NB) and coumarin (CMR) hydrogels.* Dynamic time sweep measurements showing representative data for the polymerization and degradation of NB hydrogels in response to (A) 365 nm and (B) 400 – 500 nm light irradiation and CMR hydrogels in response to (C) 365 nm and (D) 400 – 500 nm light irradiation. Measurements were conducted with a 1% strain and a frequency of 2 rad s^{-1}, within the linear viscoelastic region for these hydrogels. The light was turned on after a 30 min polymerization time, time observed to be sufficient for complete gelation of all formulations, where timeframes in which samples were irradiated are shown with the purple and blue shaded regions (I_0 = 4 mW cm^{-2} at 365 nm and I_0 = 6.7 mW cm^{-2}).

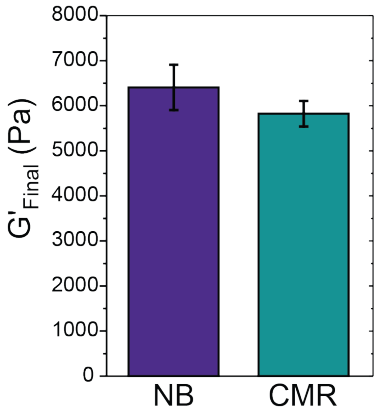

Figure S3. *Final mechanical properties after polymerization of NB and CMR hydrogels.* The final storage modulus of *in situ* formed NB and CMR hydrogels were statistically the same as determined using shear rheology. The data shown illustrate the mean (n = 6) with error bars representing standard error. The final mechanical properties of the NB and CMR hydrogels were found to be statistically the same as determined using a Student's t-test with p = 0.05.

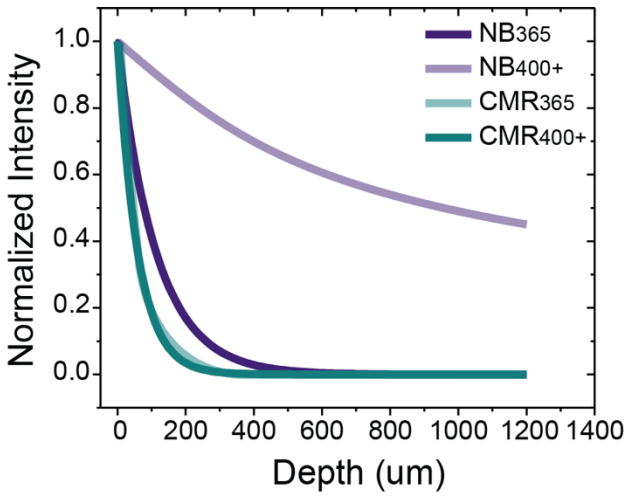

Figure S4. *Normalized intensity over hydrogel depth for thick bulk hydrogel samples.* The intensity of light transmitted through a thick hydrogel (h = 1.2 mm) samples for NB and CMR hydrogels irradiated with either 365 nm or 400 – 500 nm light for degradation. The intensity profiles were calculated as function of depth using the Beer-Lambert law. The complete attenuation of light within the NB_{365}, CMR_{365}, and CMR_{400+} formulations leads to a degradation mechanism dominated by surface erosion; alternatively, more than 40% of the light applied to the NB_{400+} gels was transmitted through the sample leading to a mechanism dominated by bulk degradation.

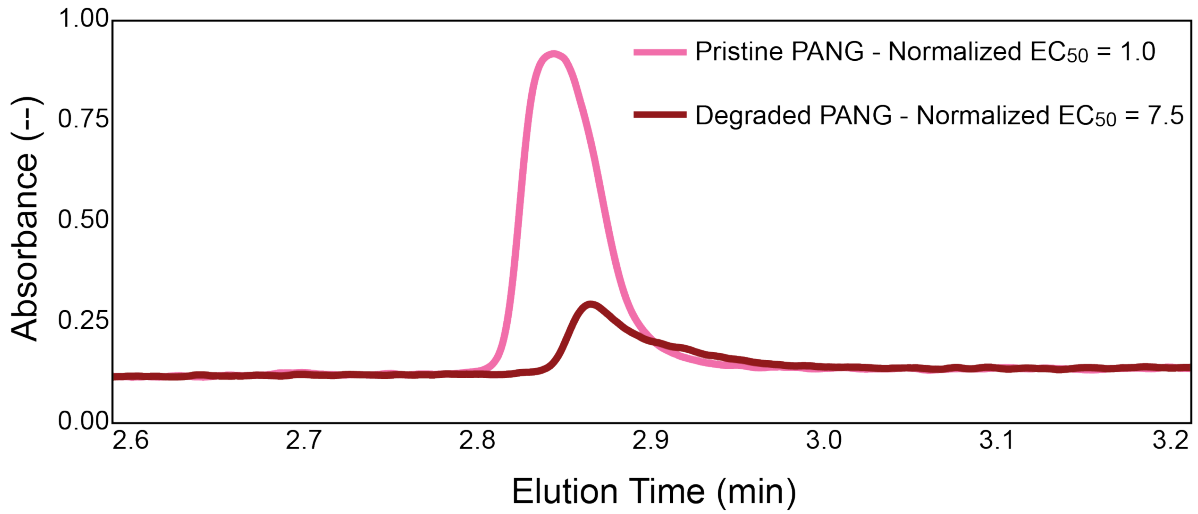

Figure S5. *Comparison of RPC traces for pristine and degraded/heat-inactivate PANG.* Representative RPC elution curves for pristine and degraded/heat-inactivated PANG traces. While both samples were loaded onto the column at theoretically the same concentration of PANG, different concentrations were observed in the RPC traces. Consequently, samples for running the lethal toxin assay were prepared to be at the same concentration based on the concentrations determined by RPC. Even still, the bioactivity of these two control samples (pristine vs. degraded/heat-inactivated) was found to be significantly different. Taken together the RPC and lethal toxin assay observations confirm that PANG remains bioactive upon encapsulation and release from NB and CMR hydrogel formulations.

Table S1. *Photodegradation rates for NB and CMR hydrogels and associated light absorbance properties.* Hydrogels were irradiated with either 365 nm (I_0 = 4 mW cm^{-2}) or 400 – 500 nm (I_0 = 6.7 mW cm^{-2}) light for degradation. The first order effective rate constants, determined from rheological data, were normalized to the incident light intensity applied to the hydrogels for fair comparison across compositions and conditions. The molar absorptivity for NB and CMR linkers that were integrated within these hydrogels were measured with UV-vis spectrophotometry, shown here for the different wavelengths that are associated with the light applied to the samples (365 nm or 400-500 nm [containing mercury arc lamp emission bands at 405 and 435 nm]).

	Irradiation Wavelength (nm)	k_{eff}/I_0 x 10^4 (cm^2 mW^{-1} s^{-1})	Molar Absorptivity (M^{-1} cm^{-1})
NB	365	9.3 ± 0.1	3940
	405	1.64 ± 0.05	880
	435		80
CMR	365	7 ± 1	8240
	405	5.2 ± 0.4	16140
	435		5520

Table S2. *Results from Tukey's comparison test for final timepoint of thick bulk hydrogel photodegradation*. Statistical comparison of normalized volume of bulk NB or CMR containing hydrogels after 20 min of irradiation with 365 nm (I_0 = 10 mW cm^{-2}) or 400 – 500 nm (I_0 = 17.1mW cm^{-2}) light. * $p < 0.05$, ** $p < 0.01$, *** $p < 0.005$, **** $p < 0.001$, and n.s. indicates not significant.

			Significance	p-value
NB_{365nm}	vs.	NB_{400+nm}	****	$p < 0.001$
NB_{365nm}	vs.	CMR_{365nm}	***	$p = 0.003$
NB_{365nm}	vs.	CMR_{400+nm}	n.s.	$p = 0.2$
NB_{400+nm}	vs.	CMR_{365nm}	***	$p = 0.001$
NB_{400+nm}	vs.	CMR_{400+nm}	****	$p < 0.001$
CMR_{365nm}	vs.	CMR_{400+nm}	n.s.	$p = 0.09$

Table S3. *Results from Tukey's comparison test for final timepoint of thick bulk hydrogel photodegradation through pig skin*. Statistical comparison of normalized volume of NB or CMR containing hydrogels after 60 min of irradiation with 365 nm (I_0 = 10 mW cm^{-2}) or 400 – 500 nm (I_0 = 17.1 mW cm^{-2}) light through a thin layer of pig skin. * $p < 0.05$, ** $p < 0.01$, *** $p < 0.005$, **** $p < 0.001$, and n.s. indicates not significant.

			Significance	p-value
NB_{365nm}	vs.	NB_{400+nm}	**	$p = 0.006$
NB_{365nm}	vs.	CMR_{365nm}	n.s.	$p = 0.5$
NB_{365nm}	vs.	CMR_{400+nm}	n.s.	$p = 0.8$
NB_{400+nm}	vs.	CMR_{365nm}	*	$p = 0.05$
NB_{400+nm}	vs.	CMR_{400+nm}	*	$p = 0.02$
CMR_{365nm}	vs.	CMR_{400+nm}	n.s.	$p = 0.9$

Table S4. *Results from Tukey's comparison test for PANG released from thick NB and CMR hydrogels*. Statistical comparison of the amount of PANG released from NB and CMR hydrogels irradiated with 365 nm (I_0 = 10 mW cm^{-2}) or 400 – 500 nm (I_0 = 17.1 mW cm^{-2}) light at various time points during light exposure. * $p < 0.05$, ** $p < 0.01$, *** $p < 0.005$, **** $p < 0.001$, and n.s. indicates not significant.

				Significance	p-value
t = 2.5 min	NB_{365nm}	vs.	NB_{400+nm}	****	$p < 0.001$
	NB_{365nm}	vs.	CMR_{365nm}	n.s.	$p = 0.2$
	NB_{365nm}	vs.	CMR_{400+nm}	n.s.	$p = 0.3$
	NB_{400+nm}	vs.	CMR_{365nm}	***	$p = 0.001$
	NB_{400+nm}	vs.	CMR_{400+nm}	****	$p < 0.001$
	CMR_{365nm}	vs.	CMR_{400+nm}	n.s.	$p = 1$
t = 5 min	NB_{365nm}	vs.	NB_{400+nm}	****	$p < 0.001$
	NB_{365nm}	vs.	CMR_{365nm}	n.s.	$p = 0.4$
	NB_{365nm}	vs.	CMR_{400+nm}	n.s.	$p = 0.1$
	NB_{400+nm}	vs.	CMR_{365nm}	***	$p = 0.003$
	NB_{400+nm}	vs.	CMR_{400+nm}	**	$p = 0.01$
	CMR_{365nm}	vs.	CMR_{400+nm}	n.s.	$p = 0.8$
t = 7.5 min	NB_{365nm}	vs.	NB_{400+nm}	****	$p < 0.001$
	NB_{365nm}	vs.	CMR_{365nm}	n.s.	$p = 0.4$
	NB_{365nm}	vs.	CMR_{400+nm}	n.s.	$p = 0.09$
	NB_{400+nm}	vs.	CMR_{365nm}	***	$p = 0.004$
	NB_{400+nm}	vs.	CMR_{400+nm}	*	$p = 0.02$
	CMR_{365nm}	vs.	CMR_{400+nm}	n.s.	$p = 0.7$
t = 10 min	NB_{365nm}	vs.	NB_{400+nm}	***	$p = 0.002$
	NB_{365nm}	vs.	CMR_{365nm}	n.s.	$p = 0.4$
	NB_{365nm}	vs.	CMR_{400+nm}	n.s.	$p = 0.06$
	NB_{400+nm}	vs.	CMR_{365nm}	*	$p = 0.02$
	NB_{400+nm}	vs.	CMR_{400+nm}	n.s.	$p = 0.1$
	CMR_{365nm}	vs.	CMR_{400+nm}	n.s.	$p = 0.5$

Table S5. *Results from Tukey's comparison test of lethal toxin assay EC50 results*. Statistical comparison of EC_{50} values measured for PANG released from NB and CMR hydrogels irradiated with 365 nm (I_0 = 10 mW cm^{-2}) or 400 – 500 nm (I_0 = 17.1 mW cm^{-2}) light. Not significant represented as n.s. as determined using a p = 0.05.

			Significance	p-value
PANG	vs.	NB_{365nm}	n.s.	p = 0.2
PANG	vs.	NB_{400+nm}	n.s.	p = 0.1
PANG	vs.	CMR_{365nm}	n.s.	p = 0.2
PANG	vs.	CMR_{400+nm}	n.s.	p = 0.2
NB_{365nm}	vs.	NB_{400+nm}	n.s.	p = 1
NB_{365nm}	vs.	CMR_{365nm}	n.s.	p = 1
NB_{365nm}	vs.	CMR_{400+nm}	n.s.	p = 1
NB_{400+nm}	vs.	CMR_{365nm}	n.s.	p = 1
NB_{400+nm}	vs.	CMR_{400+nm}	n.s.	p = 1
CMR_{365nm}	vs.	CMR_{400+nm}	n.s.	p = 1

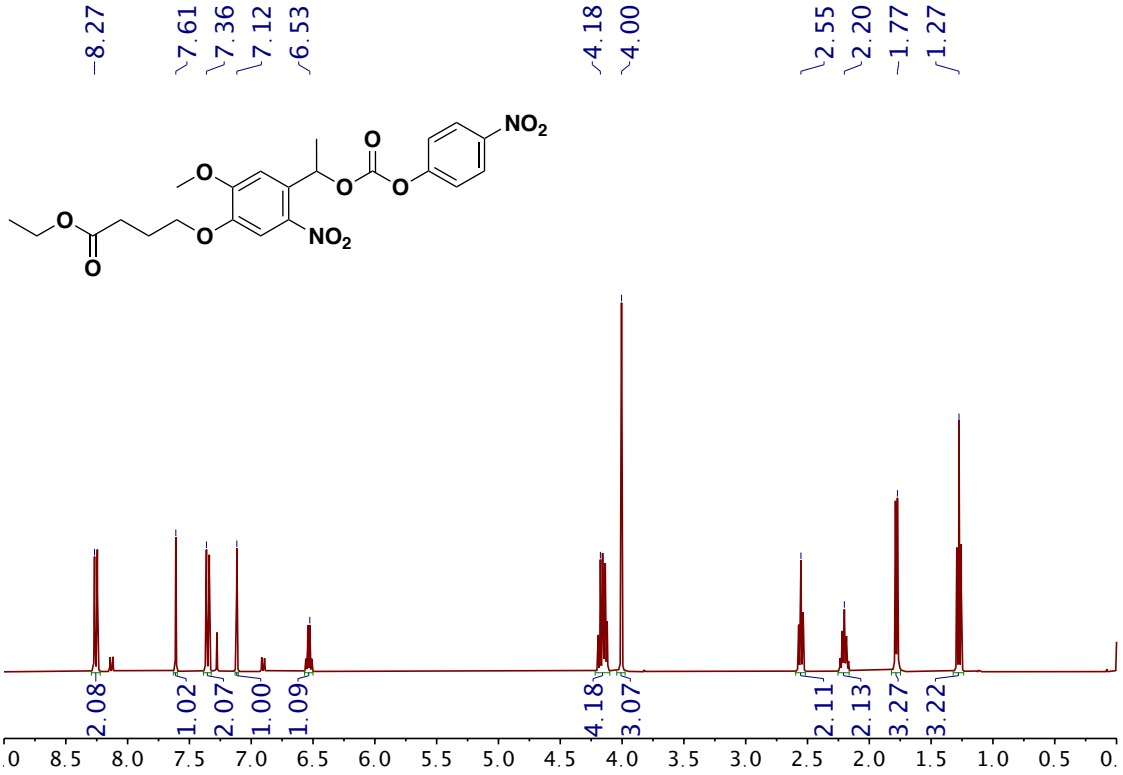

Figure S6. *NMR of compound 1.* ^{1}H NMR (600 MHz) spectra for **compound 1** in DMSO-d_6.

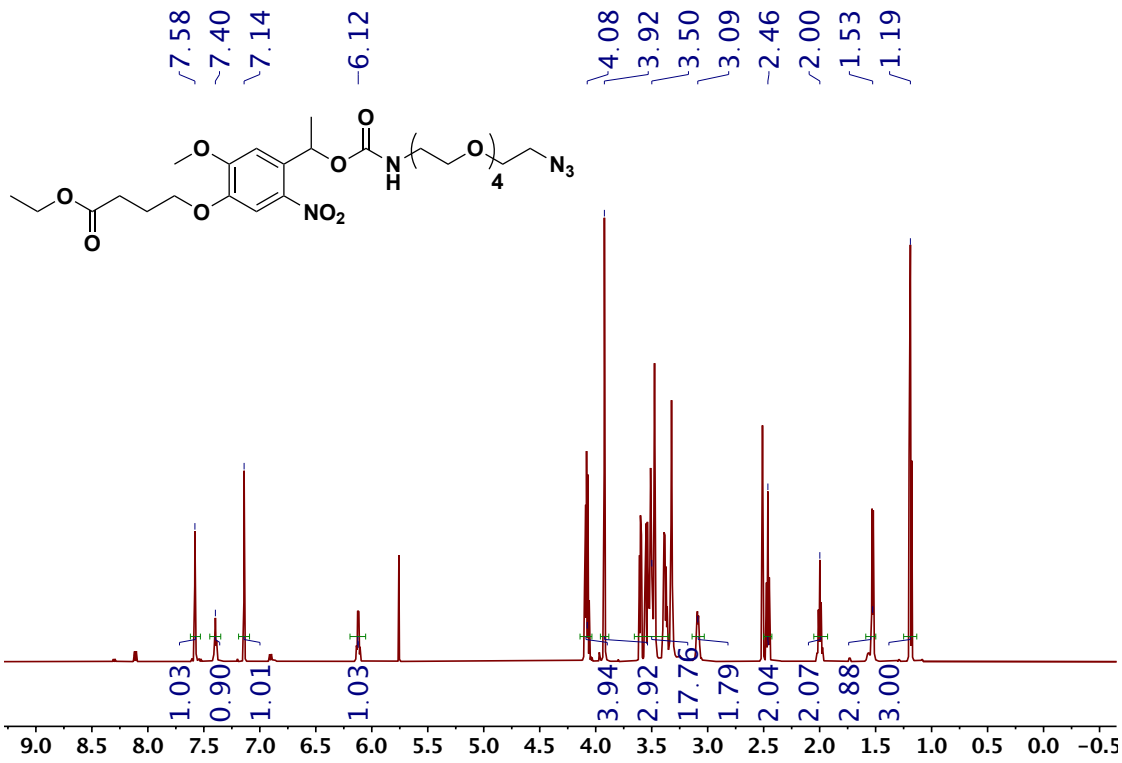

Figure S7. *NMR of compound 2.* ^{1}H NMR (600 MHz) spectra for **compound 2** in DMSO-d_6.

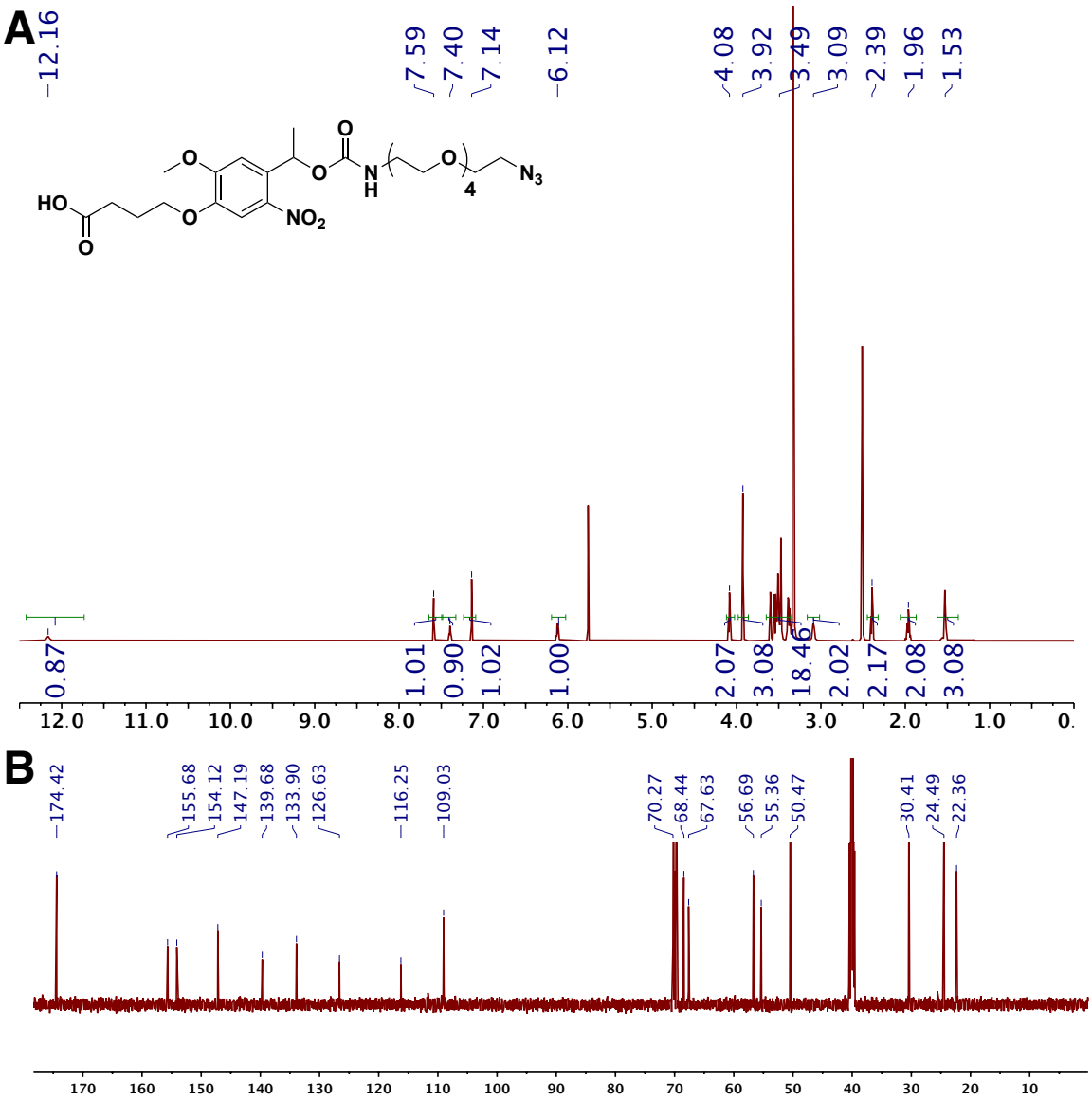

Figure S8. *NMR of NB-azide.* (A) ^{1}H NMR (600 MHz) and (B) ^{13}C NMR (151 MHz) spectra for NB-azide (**compound 3**) in DMSO-d_6.

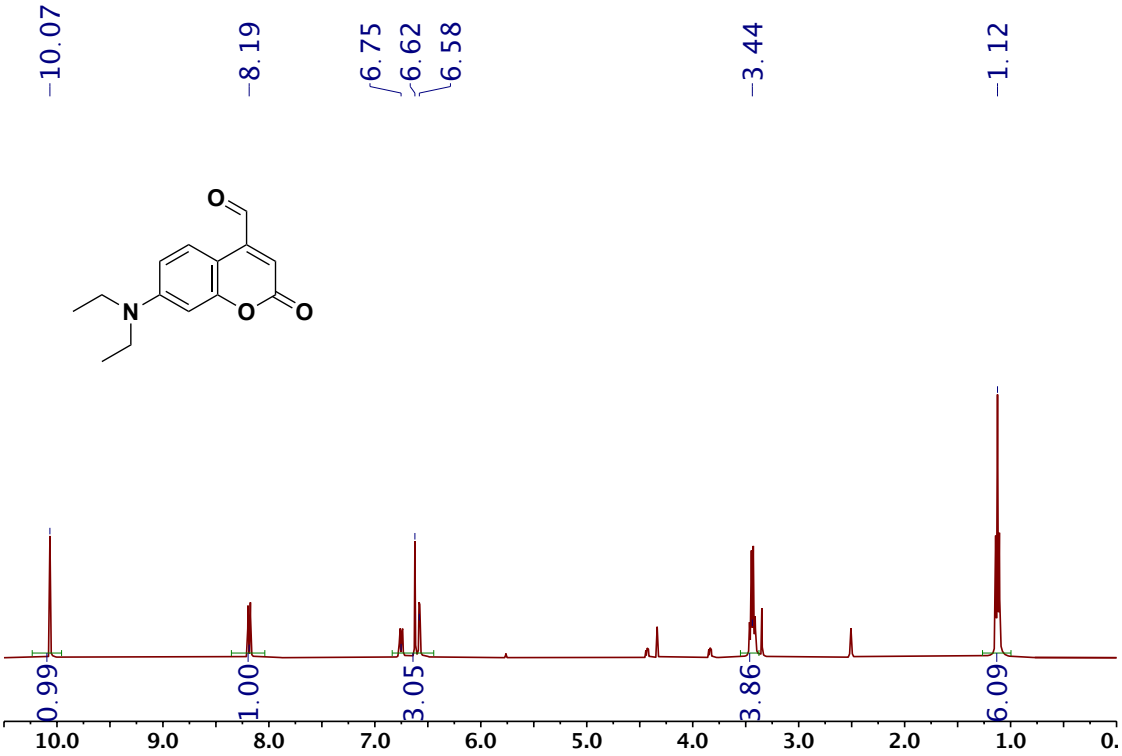

Figure S9. *NMR of compound 4.* ^{1}H NMR (600 MHz) spectra for **compound 4** in DMSO-d_6.

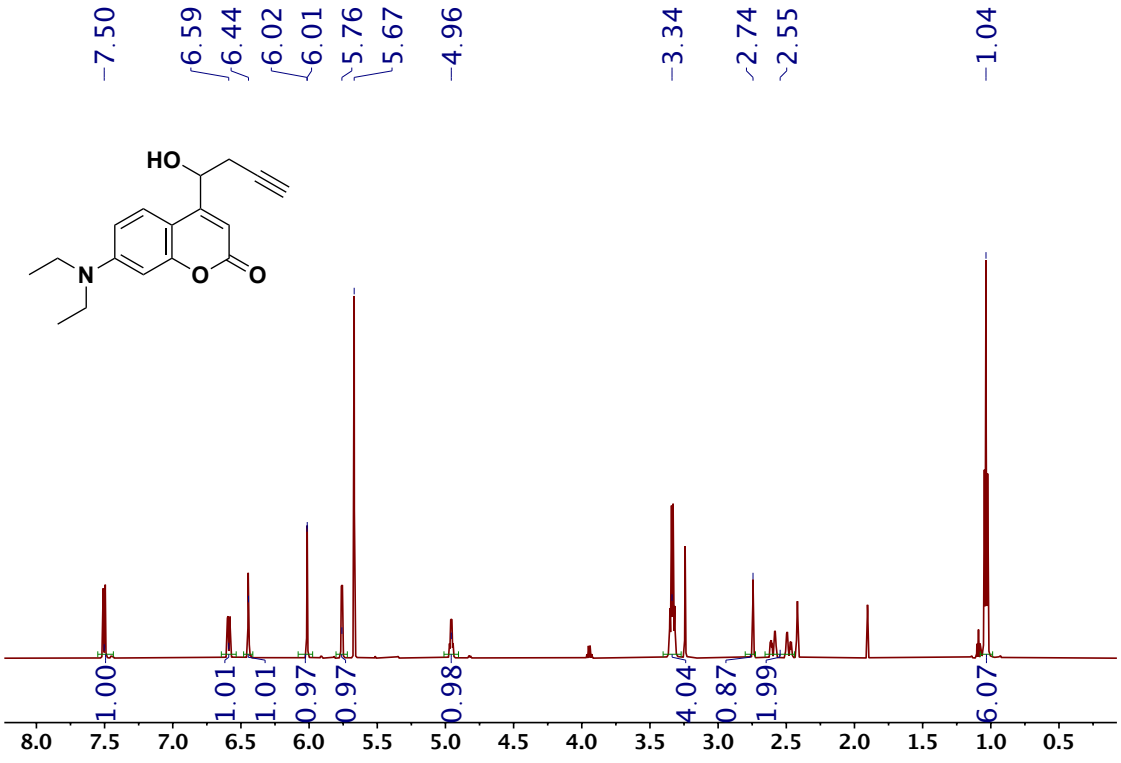

Figure S10. *NMR of compound 5.* ^{1}H NMR (600 MHz) spectra for **compound 5** in DMSO-d_6.

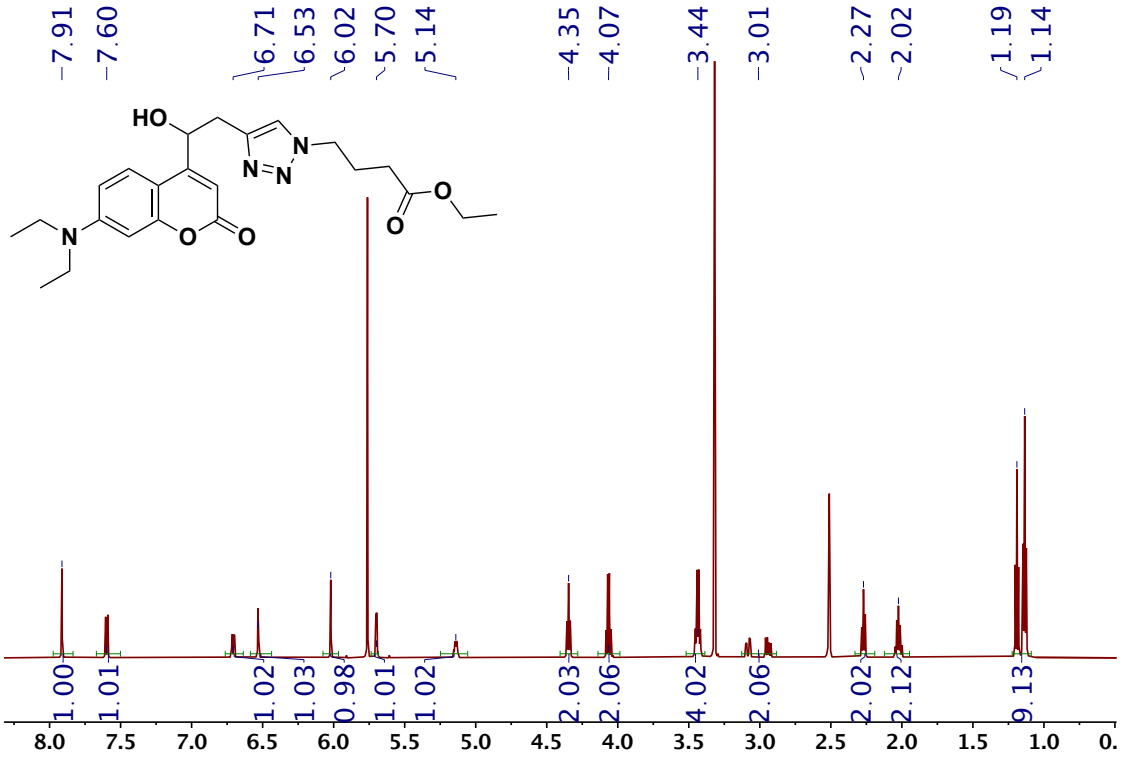

Figure S11. *NMR of compound 6.* ^{1}H NMR (600 MHz) spectra for **compound 6** in DMSO-d_6.

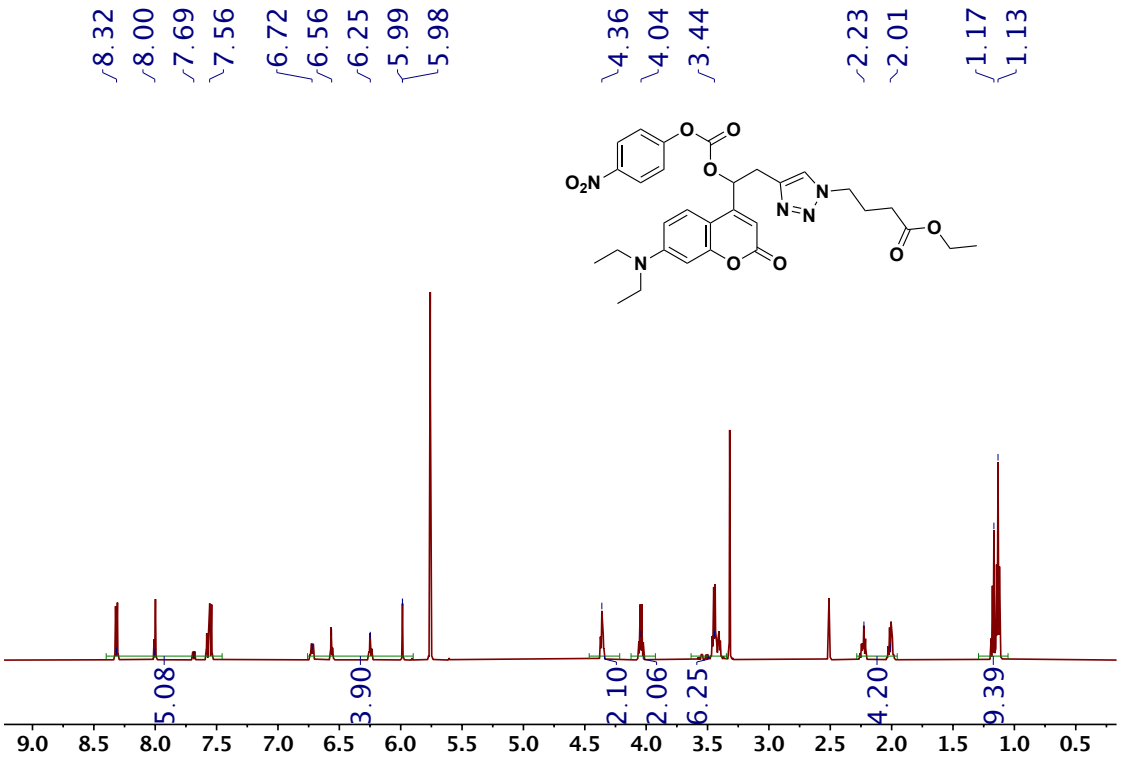

Figure S12. *NMR of compound 7.* ^{1}H NMR (600 MHz) spectra for **compound 7** in DMSO-d_6.

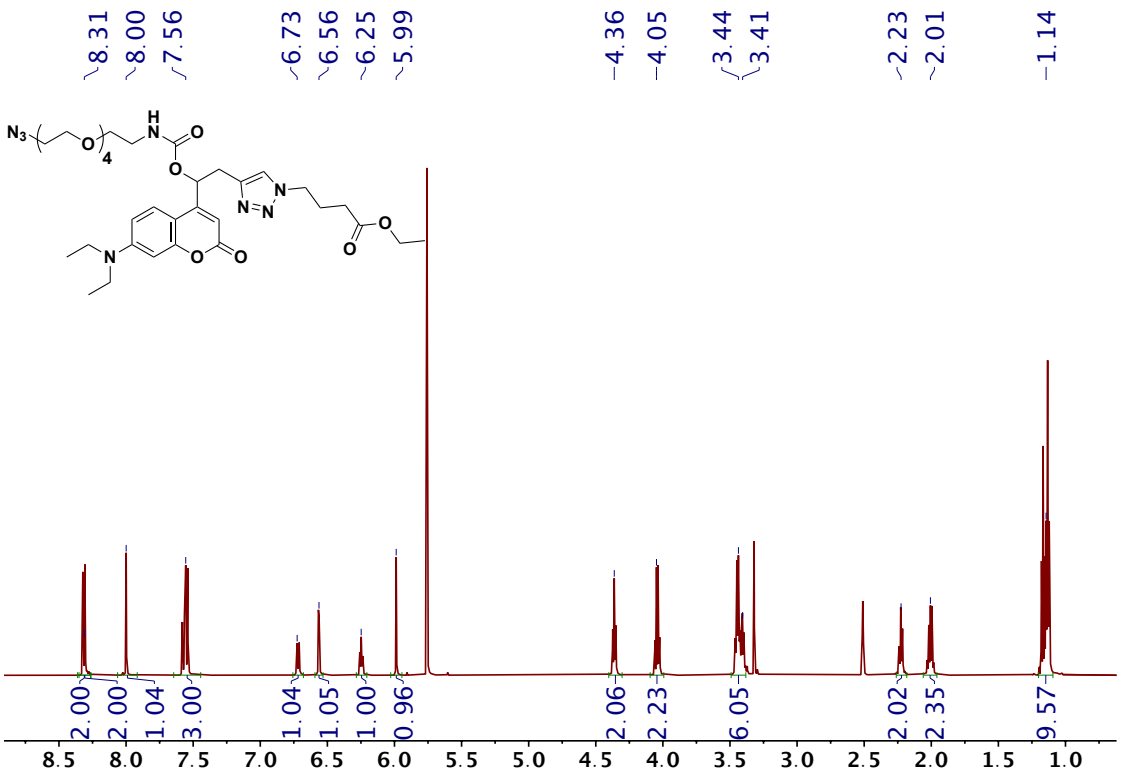

Figure S13. *NMR of compound 8.* ^{1}H NMR (600 MHz) spectra for **compound 8** in DMSO-d_6.

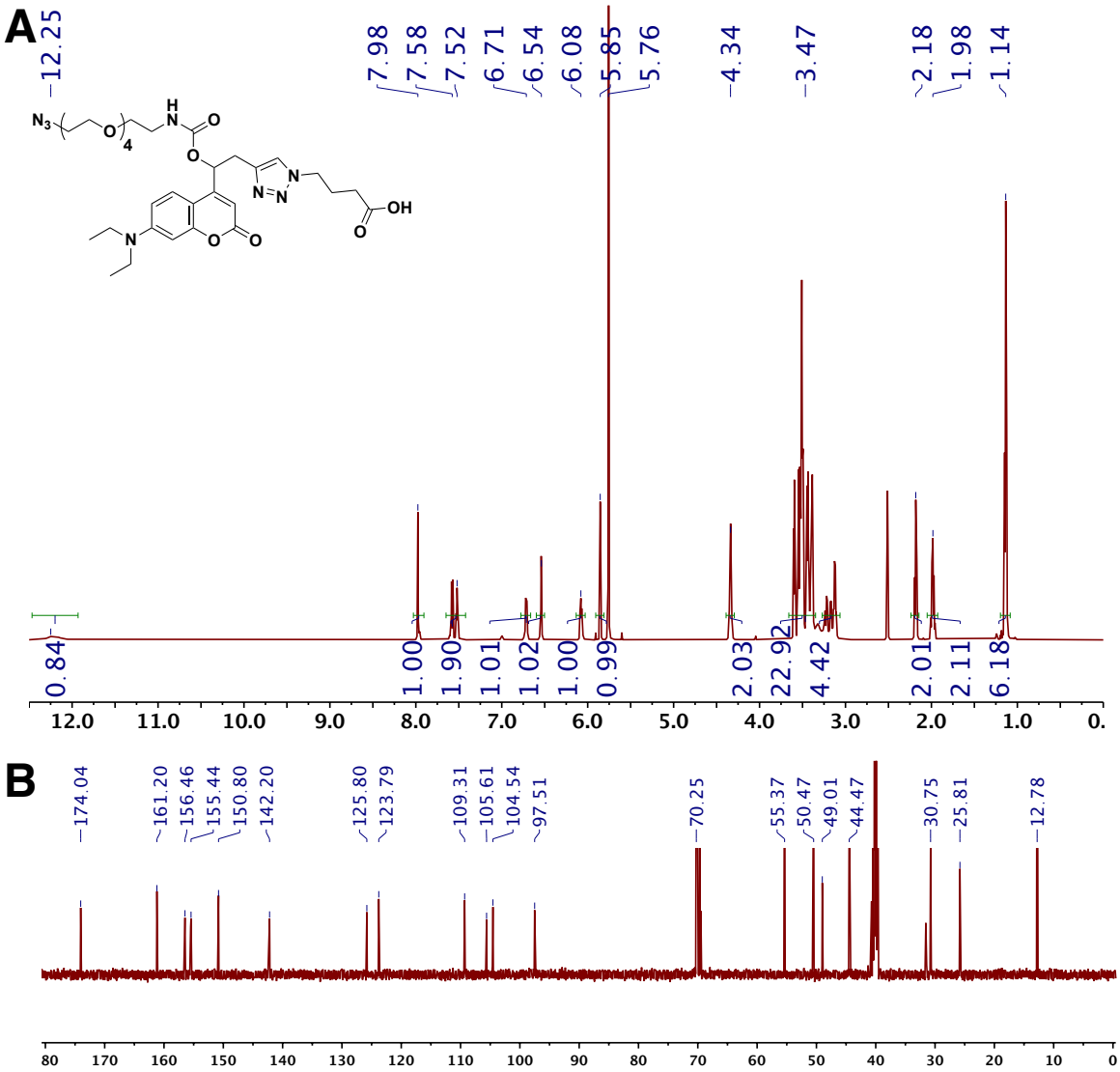

Figure S14. *NMR of CMR-azide.* (A) ^{1}H NMR (600 MHz) and (B) ^{13}C NMR (151 MHz) spectra for CMR-azide (**compound 9**) in DMSO-d_6.

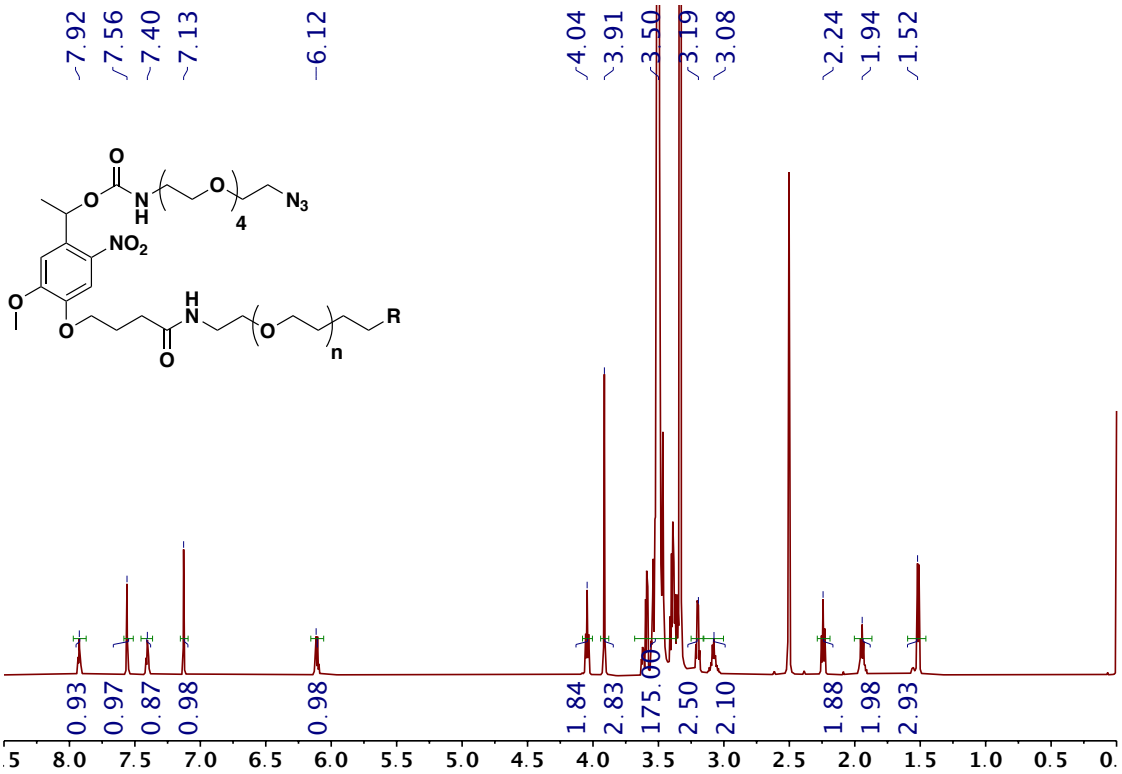

Figure S15. *NMR of PEG-di-NB-azide.* ^{1}H NMR spectrum for PEG-*di*-NB-azide (600 MHz, DMSO-d_6, 128 scan).

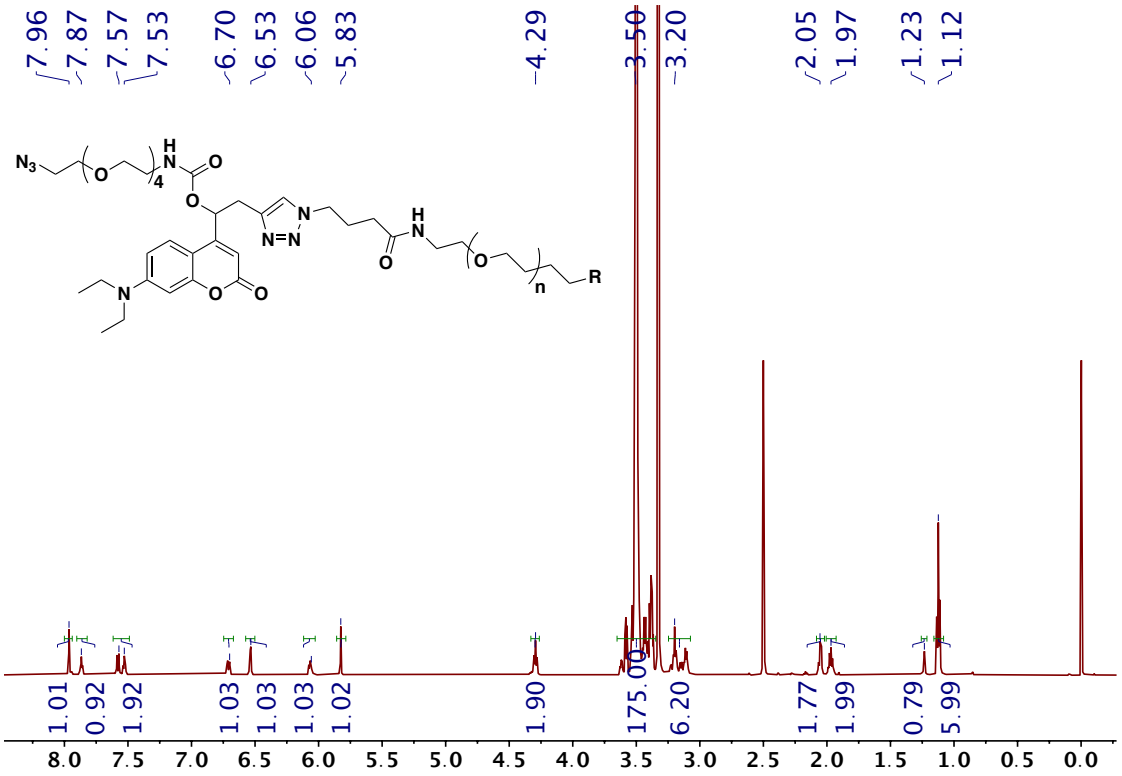

Figure S16. *NMR of PEG-di-CMR-azide.* ^{1}H NMR spectrum for PEG-*di*-CMR-azide (600 MHz, DMSO-d_6, 128 scan).

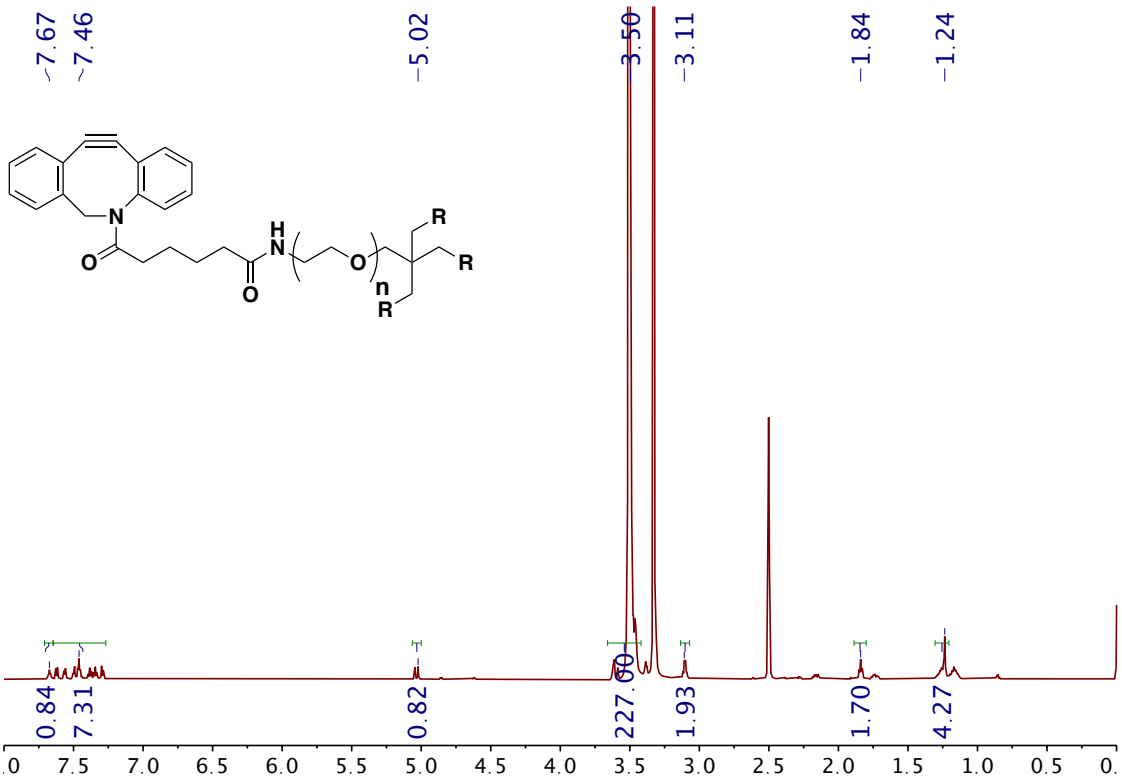

Figure S17. *NMR of PEG-4-DBCO.* ^{1}H NMR spectrum for PEG-4-DBCO (600 MHz, DMSO-d_6, 128 scan).